

PERFORMANCE COMPARISON OF THE ORDINARY AND HIGH STRENGTH STEEL REINFORCED CONCRETE FRAMES AGAINST EARTHQUAKES

A. U. Qazi, L. P. Ye*, M. B. Sharif, A. Hameed, N.M. Khan

Civil Engineering Department, U.E.T., Lahore

*Tsinghua University, Beijing, China.

ABSTRACT: Formations of collapse mechanisms under strong ground motions are not uncommon in RC frames. Failure mechanisms in ordinary RC frames can be prevented by adopting strong column weak beam philosophy. Limited flexural strength and lateral deformation capacity of the RC columns often results in the incipient of the failure mechanisms. Large inelasticity at the column base causes instability problem and structural safety is endangered. Furthermore, large residual deformations at the end of an earthquake event cannot be ruled out. A study on the performance of RC frames reinforced with high strength reinforcement in columns and ordinary reinforcements in beams revealed more steady performance as compared to ordinary RC frames. Experimental study on two bays three story frames reinforced with similar reinforcement pattern revealed more stable response at large lateral displacements. Simple replacement of ordinary steel in the column of RC frames and with the absence of yielding in columns passive frame mechanism can be demonstrated.

Key words: Earthquake; Failure mechanisms; Residual displacements; High strength steel reinforcements; Steady response.

INTRODUCTION

In the performance based design, although the structures are designed for the desired performance. However, formation of failure mechanisms and large residual displacements in the structures eventually survived from strong ground motions are not uncommon (Fischer and Li 2003). The strong column and weak beam concept in RC frame ensure that plastic hinges are confined to the beam ends and at the base of the first story columns. Plastic hinges at the columns base are necessary to initiate frame sway (Paulay and Priestley 1992). Use of un-bonded post tensioned steel tendons is common in structural systems with self centering capabilities. Many researchers have studied its use in various types of construction such as in pre-cast concrete by Priestley et al (1999), El-Sheikh et al (1999) and Kurama et al (1999), in partially pre-stressed concrete for bridge piers by Zatar and Mutsuyoshi (2002), in un-bonded post tensioned bridge piers by Kawan and Billington (2003) and in steel structures by Ricles et al (2001). Concrete ductility with fiber reinforced polymer (FRP) tendons has been studied by Naaman and Jeong (1995), Alsayed and Alhozaimy (1999) as well as hybrid FRP reinforcement by Harris et al (1998). With the development in the Engineered Cementitious Composites (ECC), a frame system with intrinsic collapse prevention capabilities has also been proposed by Fischer and Li (2003) by utilizing ECC and FRP reinforcement in columns. Besides reduced residual displacements, frame showed absence of potential collapse mechanism by avoiding yielding at the column base sections. However,

ECC being a new innovative material and is scarcely introduced to construction industry. It is still desired to explore cheaper materials and to investigate the conventional materials in achieving total mechanism with minimum residual displacements.

Ordinary steel reinforcements have limited strength and elastic deformation capacity. Consequently, flexural strength of the RC columns at the base sections is normally approached when steel yields. Flexural stiffness also deteriorates after excessive yield excursion under cyclic loadings. Eventually formations of collapse mechanisms are inevitable under large lateral sways. Rehabilitation and strengthening demands are also emerged with the excessive yielding of the reinforcements in the columns. In order to provide large lateral strength and deformation capacity to ordinary RC frames (OF), high strength steel reinforcements in RC frame columns are studied here. It is anticipated that with the use of high strength reinforcements response of the OF can be passively controlled. Hence, for seismic response comparison, two 2-bays three story reinforced concrete frames are tested with static inverted triangular reversed cyclic loading. Both the frames have same geometric details. Reinforcement area ratios and material strength properties are also kept the same. In the following discussion, test frame which is reinforced with high strength steel reinforcements in columns is abbreviated as PFT while, OF is named as OFT.

Frames geometric and reinforcement details: Geometric and reinforcement details of both the frames are shown in Fig. 1.

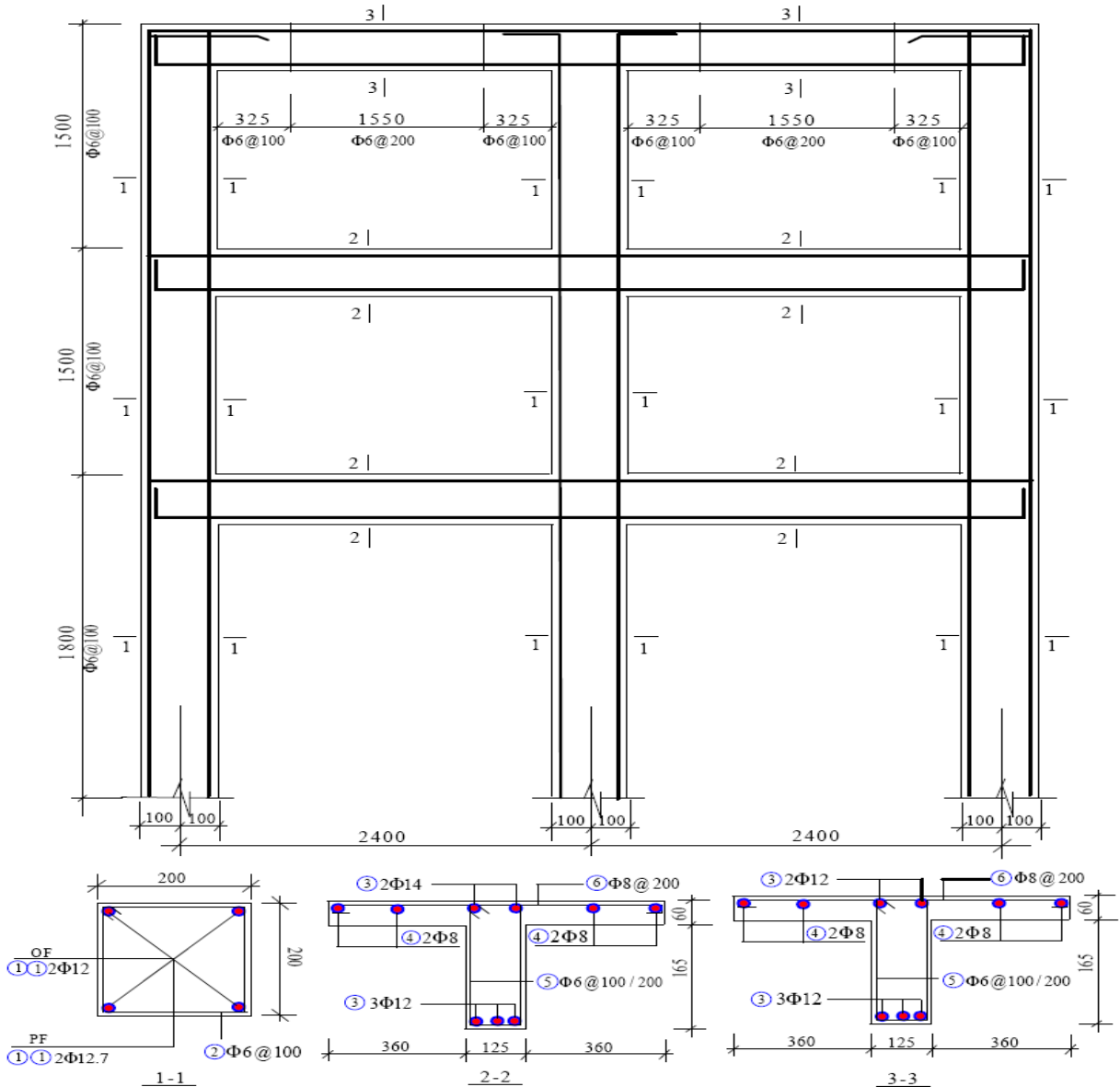


Figure 1: Frames geometric along with longitudinal and cross-sectional reinforcement details

For determining concrete compressive strength in frames, six cubes of 150x150x150mm size were filled from the same concrete batch and tested. Compressive strengths of cubes at 28 days are given in Table 1.

Table 1: Concrete strength from cubes for OFT and PFT

| Cube No. | 1 | 2 | 3 | 4 | 5 | 6 |
|------------------------------|-------|------|------|------|------|------|
| Load (kN) | 628 | 548 | 606 | 624 | 456 | 618 |
| Cubic Strength (MPa) | 27.9 | 24.3 | 26.9 | 27.7 | 20.3 | 27.5 |
| Average Load (kN) | 580 | | | | | |
| Average Cubic Strength (MPa) | 25.76 | | | | | |

For ordinary reinforcement the strength confirmed from the average of the specimens is given in Table 2. For shear reinforcement in beams and for ties in columns of OFT and PFT, Φ6 bars are used.

Table 2: Material strength properties of ordinary steel

| Diameter | Effective Area | Yield Strength | Yield Strain | Ultimate Strength | Modulus of Elasticity |
|----------|-----------------|----------------|--------------|-------------------|-----------------------|
| mm | mm ² | MPa | | MPa | GPa |
| Φ6 | 32 | 235 | 0.001175 | 373 | 200 |
| Φ12 | 113 | 325 | 0.001625 | 445 | 200 |
| Φ14 | 154 | 330 | 0.001650 | 450 | 200 |

Modulus of elasticity calculated is 200GPa. High strength steel strands used in the columns of PFT are also tested for determining material strength properties and are summarized in Table 3.

Table 3: Material strength properties of steel strands

| Diameter | Effective Area | Yield Strength | Yield Strain | Ultimate Strength | Modulus of Elasticity |
|----------|-----------------|----------------|------------------|-------------------|-----------------------|
| mm | mm ² | MPa | 10 ⁻⁶ | MPa | GPa |
| Φ12.7 | 98.7 | 1832 | 12420 | 1980 | 198 |

Since in ACI318-08, the grade of concrete is rated by the compressive strength of cylinders with diameter 150mm by 300mm. The compressive strength thus obtained is the standard cylinder strength of the concrete concerned. Therefore, from observed average strength of cubic specimens as given in Table 1 the equivalent cylinder strength concrete can be classified as C21. The "C" stands for concrete and the 21 for standard cylinder strength in MPa. Tensile strength of concrete is approximately equal to 0.1 f_c .

Material strength properties of the tested frames are summarized in Table 4.

Ultimate concrete compressive strength is assumed as half of the peak strength of concrete. From the Table 4 it is evident that the concrete used in OFT and PFT is of same strength. The reason of keeping concrete same was to study that whether simple replacement of

ordinary steel with high strength reinforcement in columns potential benefits can be obtained. Since, large lateral displacements result in yielding at column base sections due to limited flexural strength in ordinary RC frames.

Table 4 Material strength properties of the tested frames.

| Frame | Concrete | | | | Steel | |
|-------|--------------|--------------|-------------------|--------------|---------------------|------------------------|
| | f_c MPa | f_t MPa | σ_u MPa | E_c GPa | f_y (MPa) Beam | E_s Column Gpa |
| OFT | 21 | 2 | 10 | 28 | 325 | 200 |
| PFT | 21 | 2 | 10 | 28 | 325 | 1830 |

f_c is the compressive strength of concrete.

f_t is the tensile strength of concrete.

σ_u is the ultimate strength of concrete.

f_y is the yield strength of longitudinal reinforcement.

For modulus of elasticity of concrete E_c an empirical formula in ACI318-08 as given in equation 1 is used.

$$4700\sqrt{f_c} \dots 1)$$

Test setup and measurement arrangements: Strain gauges are stitched on reinforcement to measure steel strains and on concrete surface for measuring concrete strains at critical sections. The test arrangements and the markings of steel strain gauges are shown in Fig. 2 and Fig. 3 respectively. Data of concrete strains at the columns base sections is unavailable because of the spalling of concrete at the later stages of the experiment.



Figure 2: Experimental setup of tested frames

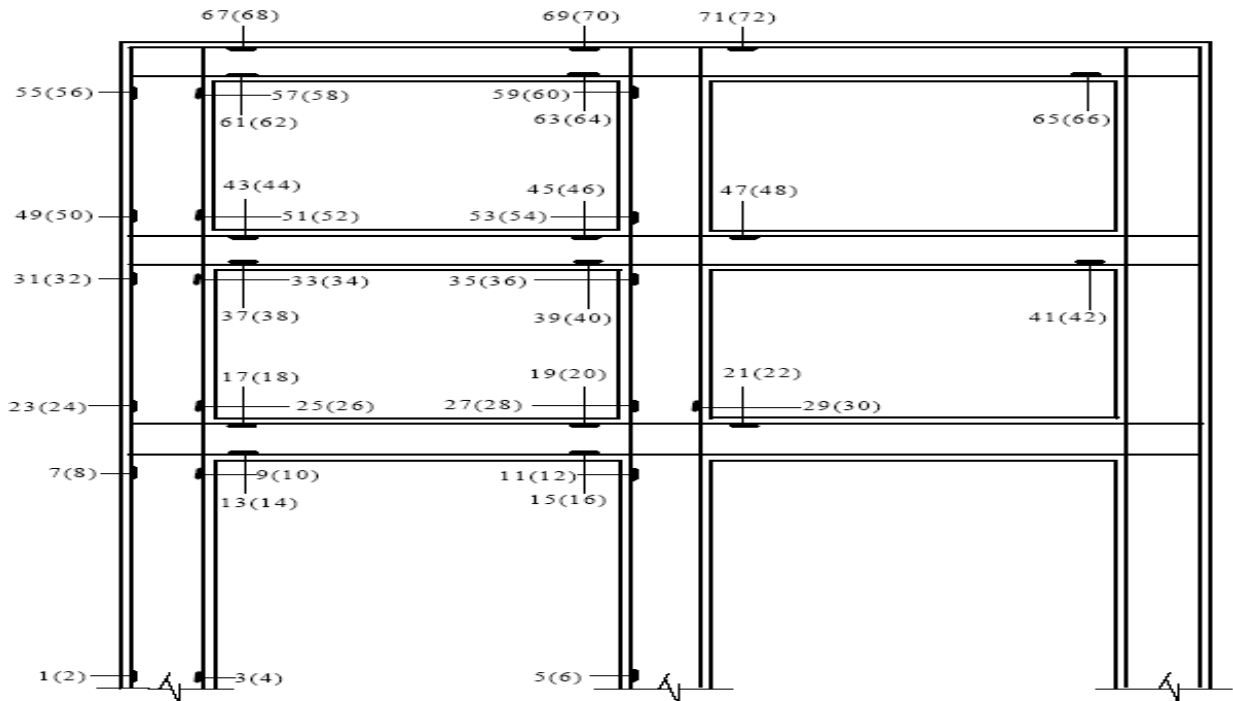


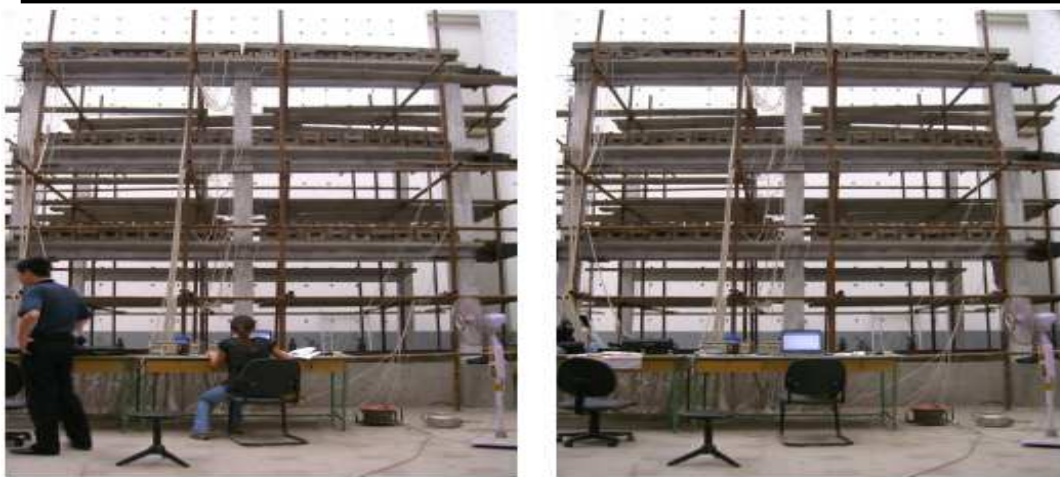
Figure 3 Marking of steel strain gauges for measuring steel strains

Loading cycles: Tests are performed under inverted triangular lateral load at first, second and third floor levels. Through hydraulically controlled actuators push and pull cycles are applied. However, for OFT after some cycles of loading, excessive yielding at the columns base sections caused difficulties in maintaining triangular load

pattern. Hence a shift in control from load to displacement control is introduced at later stages of test for OFT. The peak load and displacement magnitudes for OFT and peak load magnitudes for PFT are given in Table 5. Fig. 4(a and b) shows some of the peak lateral loading instants during the test performed on PFT.

Table 5 Loading/displacement cycle magnitudes used in tested frames

| Frames | Cycle | Load/Displacement magnitude at frame top (kN)/(mm) | | | | | | | | | |
|--------|-------|--|-----|-----|-----|-----|-----|-----|-----|------|-----|
| OFT | Load | ±5 | ±8 | ±11 | ±14 | ±17 | | | | | |
| | Disp. | ±20 | ±30 | ±40 | ±50 | ±60 | ±70 | ±80 | ±90 | ±100 | |
| PFT | Load | ±5 | ±8 | ±11 | ±14 | ±17 | ±20 | ±23 | ±26 | ±29 | ±32 |



(a) 14kN Push and Pull at frame top



(b) 26kN Push and Pull at frame top
Figure 4: Lateral loading cycles for PFT

TEST RESULTS

Observed Damage at Critical Sections in OFT and PFT: During loading frame elements are monitored carefully for recording excessive apparent damage at

critical sections. For OFT damage observed at some of the critical column base sections is shown in Fig. 5(a and b).



Figure 5 Damage photos at column base sections in OFT at ± 32kN lateral load

These pictures depict the ultimate observed damaged recorded after last loading cycles. Spalling of concrete along with scattered cracks at the columns base sections is evident. For PFT the observed damage at critical sections is also shown at the end of last two loading cycles. Fig. 6(a and b) show damage at the instant when lateral push approached 32kN load at the frame top.

While, for 32kN pull damage at the column base sections is shown in Fig. 7(a and b). Distress in concrete at the column base section is apparent from these pictures. However, excessive spalling of concrete along with opening of shear stirrups and buckling or bulging of longitudinal high strength reinforcement is not seen in PFT.

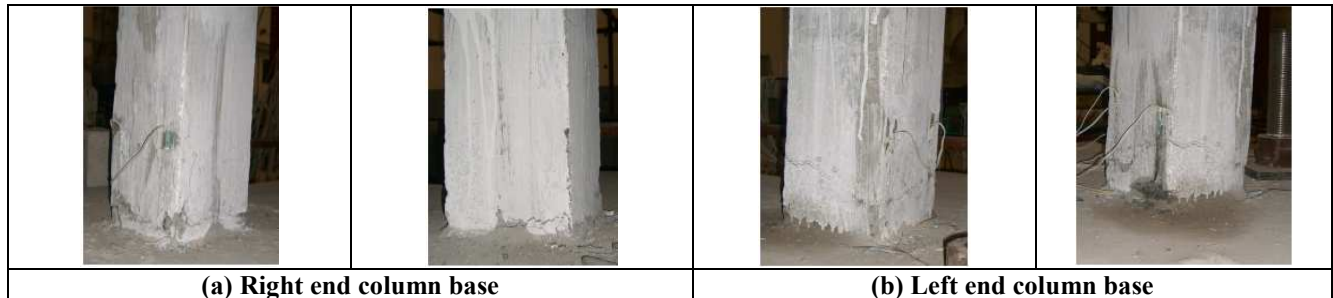


Figure 6 Damage photos at column base sections in PFT at +32kN (Push) at frame top

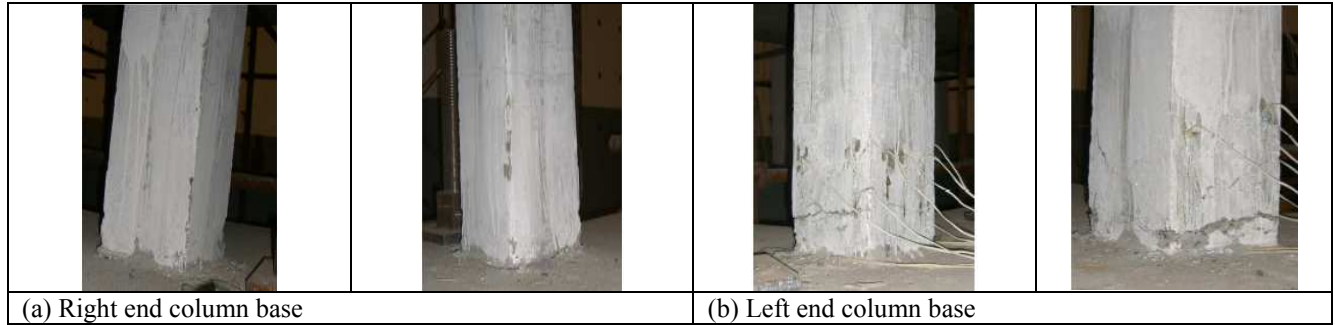


Figure 7 Damage photos at column base sections in PFT at -32kN (Pull) at frame top

Observed Strains at Critical Sections in OFT and PFT: For response comparison material strains at critical sections are recorded and are compared for OFT and PFT. For steel a total of 72 gauges are glued on reinforcements at critical sections and their markings are shown in Fig. 3. However, during the test in PFT because

of fluctuation in power some data recording lost when power restored. Hence, for comparison those critical sections where data is available for both the OFT and PFT are compared. Further, strains verses total lateral push measured at critical sections are also compared.

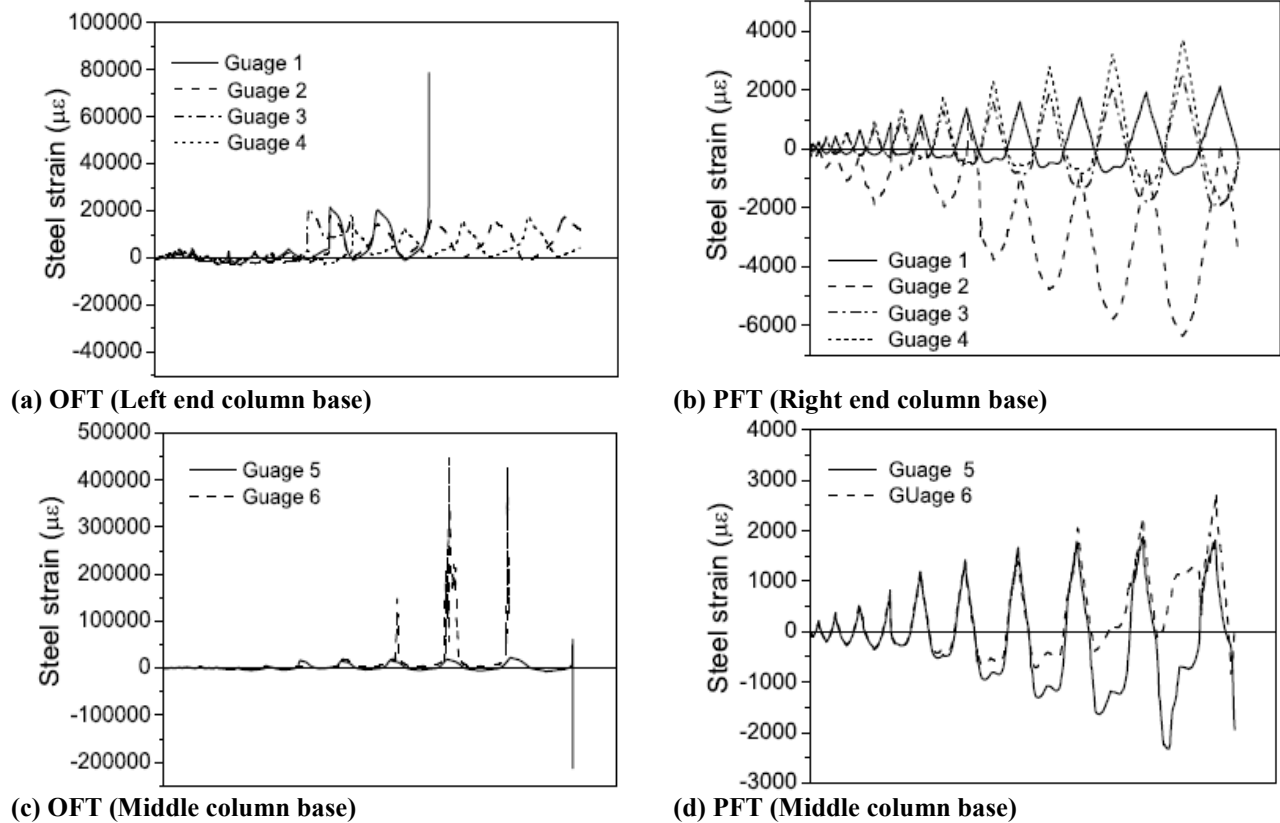
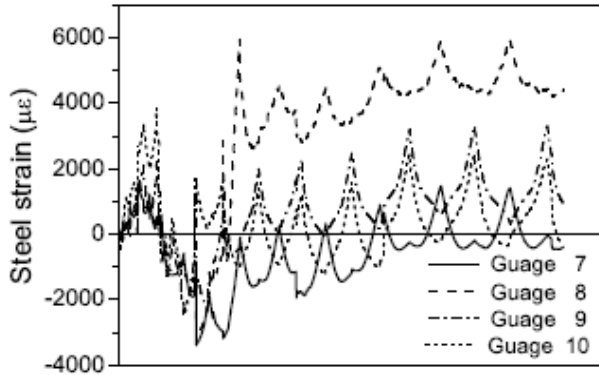


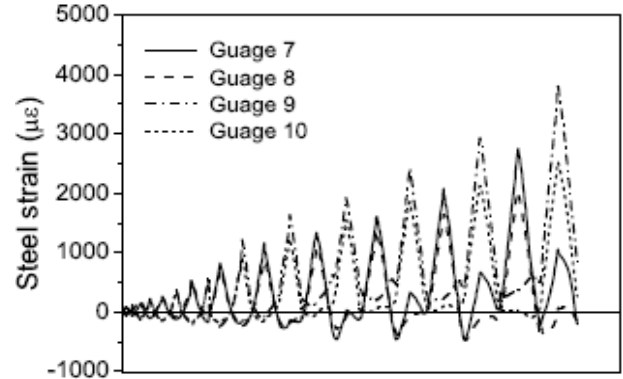
Figure 8 Steel strains measured at critical sections in OFT and PFT

Steel Strains at Critical Sections in OFT and PFT: Steel strains at critical sections are shown in Fig. 8(a to d) and in Fig. 9(a and b). Excessive yielding at the middle column base sections is also evident from the observed total strain during the test in OFT. Further strains recorded at the critical sections represent more stable

response in PFT by showing positive and negative strain magnitudes on both sides of the origin. These observations are also confirmed from the total positive load versus strains plot shown in Fig. 10(a and b). More pronounced yielding with lower lateral load magnitude is evident from strain gauge data for the OFT (Fig. 10).

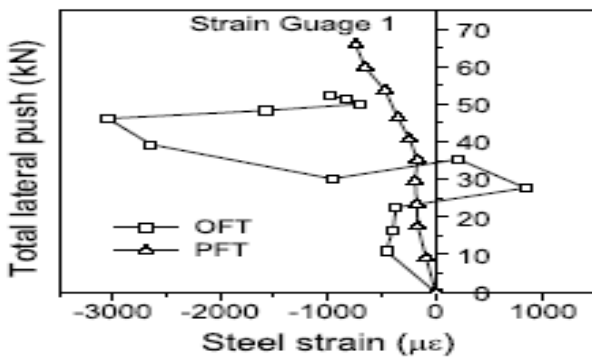


(a) OFT (Top of first story left end column)

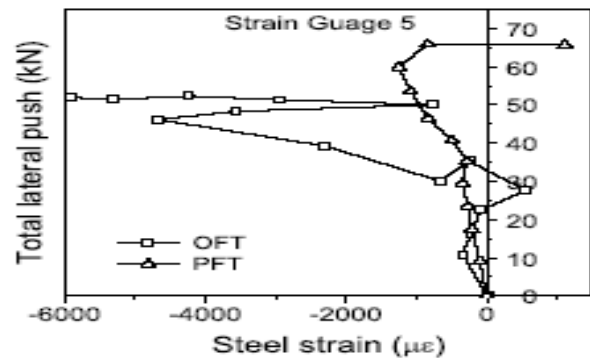


(b) PFT (Top of first story left end column)

Figure 9 Steel strains measured at critical sections in OFT and PFT



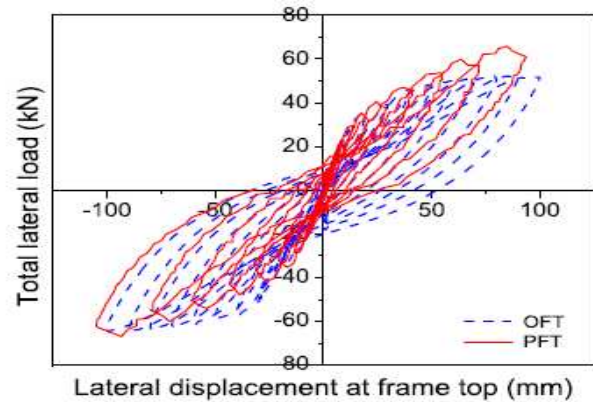
(a) Left column base



(b) At middle column base

Figure 10 Steel strains verses total lateral load measured at critical sections in OFT and PFT

Cyclic Loading Curves of OFT and PFT: OFT and PFT are laterally loaded with inverted triangular cyclic loading. In the first cycle, unloading started when the load approached 5kN at the frame top. To maintain inverted triangular load distribution, load magnitude at the second and third floor applied are 3.438kN and 1.875kN respectively. Each successive cycle is performed with a load increment of 3kN at the frame top while at second and first floor proportional increment to maintain inverted triangular loading is strictly followed. However, it is important to mention here that in case of OFT, after yield initiation at the column base sections inverted triangular lateral load control is difficult to achieve. Hence a shift from load control to displacement control adopted at the latter stages of the test and the target displacements at the frame top are given in Table 5 for OFT. This eventually resulted in some loss in reporting of the actual performance of OFT and a strict comparison between OFT and PFT becomes unattainable because of difference in load control pattern. For highlighting response difference, total lateral load verses lateral displacement at frame top is shown in Fig. 11.



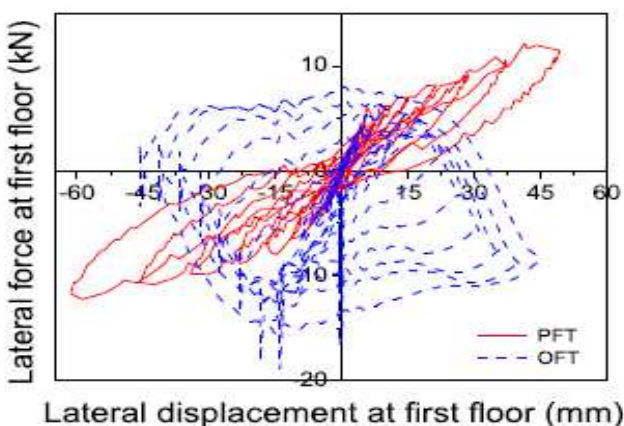
Total lateral load-displacement relation at frame top of OFT and PFT

Figure 11 Lateral displacement at frame top verses total lateral force of OFT and PFT

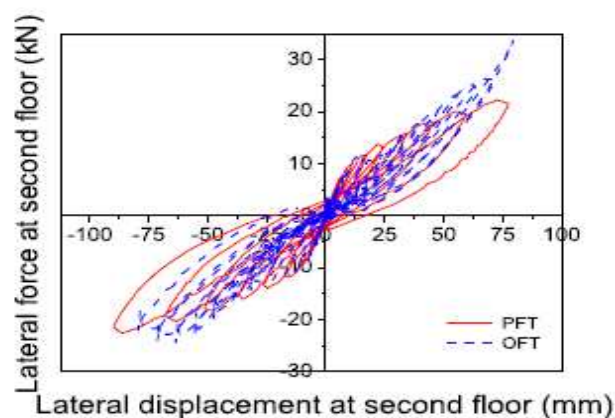
It is quite evident from the OFT curve that in third quadrant it shows more strength and less residual displacement than in the first quadrant. It is probable that less control during the test on OF caused some shift in the origin of the hysteresis curves. Fig. 12(a and b) are drawn to compare the load and displacement response at each floor level for both frames. While observing these

diagrams, it must be considered that in OFT a shift from load control to displacement control occurred in the latter stages of the test. Excessive yielding and softening

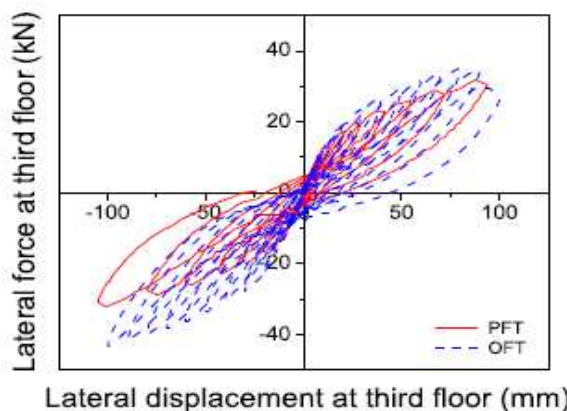
observed in OFT at the first story. While, PFT showed more stable response at all the stories.



(a) Lateral load-displacement relation at first floor of OFT and PFT



(b) Lateral load-displacement relation at second floor of OFT and PFT



(c) Lateral load-displacement relation at third floor of OFT and PFT

Figure 12 Lateral displacement versus lateral force comparison of PFT and OFT

Observed Failure Mechanism: Tests on frames reveal soft story failure mechanism in OFT while, a more stable response is observed in PFT. It can be concluded that in PFT formation of failure mechanism is delayed as compared with OFT. Proportioning of the beam column stiffness plays important role in the failure mechanism, strength and displacement response of RC frames. To achieve response benefits with PFT, beam column stiffness ratio should also be carefully controlled. In the test frames since beams are with flanges while columns are relatively thin and more flexible. Therefore, beam column stiffness is almost equal and columns are also lightly reinforced with a ratio of almost 1%. Hence, it is believed that because of lesser strength and stiffness the full contribution of columns towards response mechanism cannot be fully realized for both OFT and PFT.

Conclusions: Two bays three story ordinary and high strength steel reinforced concrete frames are compared by

test results for evaluating difference between response mechanisms. From the test results following conclusions can be drawn:

1. With high strength steel as reinforcement in frame columns more stable response at large lateral displacements can be achieved.
2. Frame failure mechanisms can be successfully controlled with high strength steel as reinforcement in columns.
3. With the use of high strength reinforcements in columns less residual drifts with comparatively large story forces can be obtained.
4. From the experimental findings, it is also inferred that the beam column stiffness ratio also plays important role in the response mechanism at large lateral sways. Since, in the test frames beams used were with flanges and columns were relatively thin and lightly reinforced. Hence, with almost equal stiffness of beam column elements full contribution

of columns cannot be fully realized for both the OFT and PFT. Lack of control during test on OFT, while bond slips and anchorage losses in PFT also hindered true realization and comparison between the frames. Before practical application of the proposed frame mechanism some other parameters which can influence the inelastic dynamic response need to be explored.

REFERENCES

- Alsayed S. H. and A.M. Alhozaimy. Ductility of concrete beams reinforced with FRP bars and steel fibers. *J. Compos. Mat.*, 33(19):1792–1806, (1999).
- El-sheikh M. T.; R. Sause and S. Pessiki. Seismic Behavior and Design of Un-bonded Post Tensioned Pre Cast Concrete Frames. *PCI Journal*, 44(3):54–71, (1999).
- Fischer G. and V. C. Li. Intrinsic response control of moment resisting frames utilizing advanced composite materials and structural elements. *ACI Struct. J.*, 100(2), 166-176, (2003).
- Harris H. G.; W. Samboonsong and F. K. Ko. New Ductile FRP Bars for Concrete Structures. *J. Compos. Cons.*, 2(1):28–37, (1998).
- Kwan W. P. and S. L. Billington. Unbonded Post-Tensioned Bridge Piers. I: Monotonic and Cyclic Analyses. *J. Bridge Eng.*, 8(2):92–101, (2003).
- Kurama Y.; S. Pessiki and R. Sause. Seismic Behavior and Design of Un-bonded Post tensioned Precast Concrete Walls. *PCI Journal*, 44(3):72–89, (1999).
- Naaman S. E. and S. M. Jeong. Structural Ductility of Concrete Beams Pre-stressed with FRP Tendons. Proceedings of Second International RILEM Symposium, Non Metallic Reinforcement for Concrete Structures, Belgium, 379-386, (1995).
- Paulay T. and M. J. N. Priestley. Seismic design of reinforced concrete and masonry buildings, Wiley, New York (1992).
- Priestley M. J. N.; S. S. Sritharan and J. R. Conley. Preliminary Results and Conclusions from PRESSS Five-Story Precast Concrete Test Building. *PCI Journal*, 44(6):42–67, (1999).
- Ricles J. M.; R. Sause and M. M. Garlock. Post Tensioned Seismic Resistant Connections for Steel Frames. *J. Struct. Eng.*, 127(2):113–121, (2001).
- Zatar W. A. and H. Mutsuyoshi. Residual Displacements of Concrete Bridge Piers Subjected to Near Field Earthquakes. *ACI Struct. J.*, 99(6):740–749, (2002).